

Theoretical Study of Intramolecular Aldol Condensation of 1,6-Diketones: Trimethylsilyl Substituent Effect

Jean-Philippe Bouillon, Charles Portella, James Bouquand, and Stéphane Humbel*

UMR 6519, Université de Reims Champagne-Ardenne/CNRS, UFR Sciences BP 1039, F-51687 REIMS Cedex 2, France

stephane.humbel@univ-reims.fr

Received June 15, 2000

Diastereoselective intramolecular aldol condensations are investigated in an experimental and computational study of 1,6-diketones. *Ab initio* results show the importance of the acid medium and disapprove the possibility of a spontaneous cyclization, even for silylated compounds. The combination of both experimental and computational approaches brings valuable information on the mechanism and on the selectivity of the aldol reaction. It is found that the enolization of the diketone is a key step in acid-catalyzed mechanism. The cyclization step bears a very small activation energy. The dehydration of the aldols are discussed.

Introduction

An aldol reaction is the reaction of one carbonyl compound, acting as a nucleophile in the form of its enol or enolate derivative, with another one, acting as an electrophile. The primary product is a β -hydroxycarbonyl compound. Under some conditions, this initial product undergoes dehydration, resulting in an α,β -unsaturated carbonyl compound.^{1,2} The general reaction is subject to either base or acid catalysis. The addition reaction of enolate (basic conditions) with carbonyl compounds is of very broad scope and great synthetic importance.³ It is also possible to carry out the aldol condensation under acidic conditions,⁴ but there is little study of its stereochemistry in these conditions. The two carbonyl compounds may or not be the same. Moreover, the carbonyl moieties may be included in the same compound as it is the case for dialdehydes, keto aldehydes, or diketones. Intramolecular aldol reactions of 1,6-dialdehydes and -diketones have been described in many reports,² most of these being base-promoted and leading directly to cyclopentenones.⁵ In this paper, we are interested mostly in 1,6-dicarbonyl compounds that are nonenolizable at the external α - and α' -carbon atoms (except for the octa-2,7-dione).

Aldol Cyclization. The first intramolecular aldol condensations were performed with bis(acylsilanes) to examine various potential synthetic applications of these

new functionalized organosilicon compounds. In view of sensitivity of bis(acylsilane) to basic conditions,⁶ the aldol reaction was mainly investigated under neutral or acidic activation. Thus, the enol form **2** (Scheme 1) is the reactive nucleophile. It can cyclize directly with the second carbonyl function via a proton transfer from the hydroxyl to the carbonyl group (Scheme 1, uncatalyzed mechanism). A protonated carbonyl tautomer **p2** would also produce first the intermediate **p4** then the aldols **4a** or **4b** after a deprotonation step (Scheme 1, acid-catalyzed mechanism). As shown in Scheme 1, two diastereomers **4a** and **4b** can in principle be formed. For each mechanism two different paths, named path a (leading to **4a**) and path b (leading to **4b**) can occur.

As previously reported,⁷ the aliphatic bis(acylsilane) **1** (R = TMS) underwent spontaneous yet very slow cyclization to the aldol **4a** (R = TMS) (45% after storage for six months in a refrigerator). Moreover, addition of a catalytic amount (10%) of *p*-toluenesulfonic acid (PTSA) to bis(acylsilane) **1** (R = TMS) and distillation in a kugelrohr apparatus gave a mixture of the aldol **4a** (R = TMS) (46%), the condensation product **5** (R = TMS) (16%), and the starting material (7%) (Scheme 2, Table 1). We obtained only the diastereomer **4a** (R = TMS). To study the effect of a trimethylsilyl group on the aldol reaction, we synthesized two other 1,6-diketones **1** with methyl (R = Me) and *tert*-butyl groups (R = *t*Bu). The octa-2,7-dione was prepared by reaction of the corresponding carboxylic acid dichloride with lithium dimethylcuprate(I) according to literature.⁸ The *tert*-butyl analogue was obtained by condensation of *tert*-butyllithium with diethyl adipate.⁹

Methyl and *tert*-butyl derivatives were thermolyzed by the same procedure using 10% of PTSA. However, the conversion was very low (39% for the methyl substituted case and 6% for the *tert*-butyl analogue, Table 1: entries 2, 4). No aldol product was detected in the crude mixture;

* To whom correspondence should be addressed. Tel: 33 (0)3 26 91 33 59. Fax: 33 (0)3 26 91 31 66.

(1) Nielsen, A. T.; Houlihan, W. J. *Org. React. (N.Y.)* **1968**, *16*, 1.

(2) Heathcock, C. H. *Comprehensive Organic Synthesis*; Trost, B. M., Ed.; Pergamon Press: New York, 1991; p 133.

(3) Carey, F. A.; Sundberg, R. J. *Advanced Organic Chemistry*, 3rd ed.; Plenum Press: New York and London, 1990, Part B, Chapter 2, p 55.

(4) (a) Baigrie, L. M.; Cox, R. A.; Slebocka-Tilk, H.; Tencer, M.; Tidwell, T. T. *J. Am. Chem. Soc.* **1985**, *107*, 3640. (b) Noyce, D. S.; Snyder, L. R. *J. Am. Chem. Soc.* **1959**, *81*, 620.

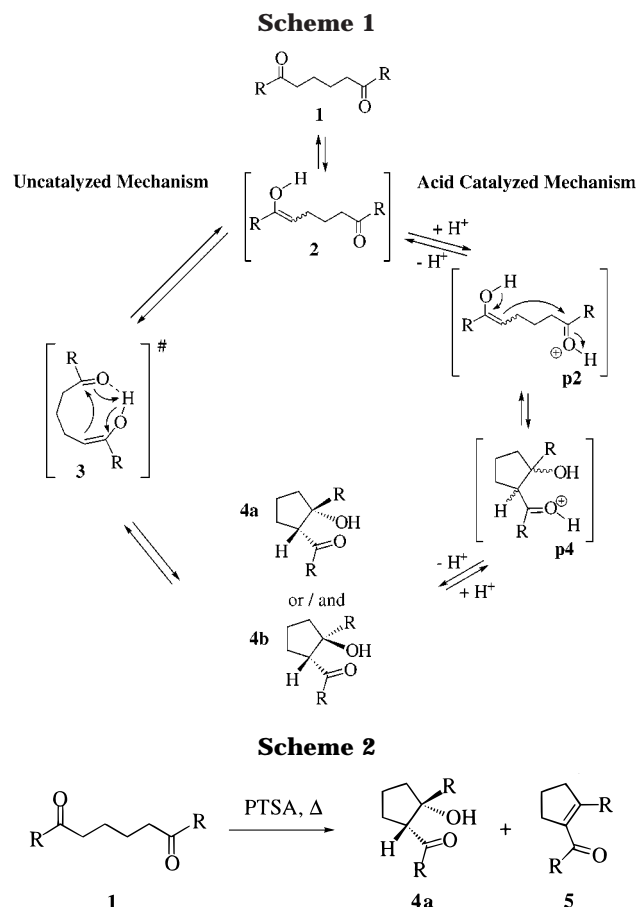
(5) (a) Brown, J. B.; Henbest, H. B.; Jones, E. R. H. *J. Chem. Soc.* **1950**, 3634. (b) Harayama, T.; Takatani, M.; Yamanaka, A.; Ikeda, H.; Ohno, M.; Inubushi, Y. *Chem. Pharm. Bull.* **1981**, *29*, 766. (c) Nakane, M.; Hutchinson, C. R. *J. Org. Chem.* **1980**, *45*, 4233. (d) Murai, A.; Tanimoto, N.; Sakamoto, N.; Masamune, T. *J. Am. Chem. Soc.* **1988**, *110*, 1985. (e) Meyer, W. L.; Wolfe, J. F. *J. Org. Chem.* **1962**, *27*, 3263. (f) Aunmiller, J. C.; Whittle, J. A. *J. Org. Chem.* **1976**, *41*, 2955.

(6) Brook, A. G. *Acc. Chem. Res.* **1974**, *7*, 77.

(7) Bouillon, J. P.; Portella, C. *Eur. J. Org. Chem.* **1999**, 1571.

(8) Posner, G. H.; Whitten, C. E.; McFarland, P. E. *J. Am. Chem. Soc.* **1972**, *94*, 5106.

(9) Petrov, A.; Sokolowa, E.; Lan, G.-C. *Bull. Soc. Chim. Fr.* **1958**, 178.

**Table 1. Thermolyses of Bis(acylsilane) and Diketones.**

entry	R	conditions PTSA (equiv)	conversion (%)	4a (%)	5 (%)
1	TMS	0.1	93	46	16
2	Me	0.1	39	—	16
3	Me	1.0	92	—	57
4	<i>t</i> Bu	0.1	6	—	—
5	<i>t</i> Bu	1.0	18	—	—

only low yield (16%) of cyclopentenone **5** (R = Me) was obtained after chromatography on silica gel. Thus, more vigorous conditions were required to efficiently induce the cyclization of diketones as compared to the bis-(acylsilane). The thermolyses were thus performed using 1 equiv of *p*-toluenesulfonic acid. In such conditions, the methyl-substituted cyclopentenone was produced in good yield (57%) whereas we still obtained only low conversion (18%) for *tert*-butyl diketone (Table 1: entries 3, 5).

These observations showed clearly the benefit effect of trimethylsilyl group on the aldol reaction. On one hand, the overall yield of aldol + cyclopentenone is significantly greater than for methyl and *tert*-butyl analogues; on the other hand, the trimethylsilyl group stabilizes the aldol product, which was obtained as the single diastereomer **4a** (R = TMS), with a *cis* relationship between the hydroxyl and the silylcarbonyl group.⁷

Computational Study

To better understand these experimental results, we performed a detailed theoretical study on both aforementioned mechanisms (Scheme 1). Our calculations intend to compare the various substituents Me, SiH₃, *t*Bu, and TMS for this reactivity.

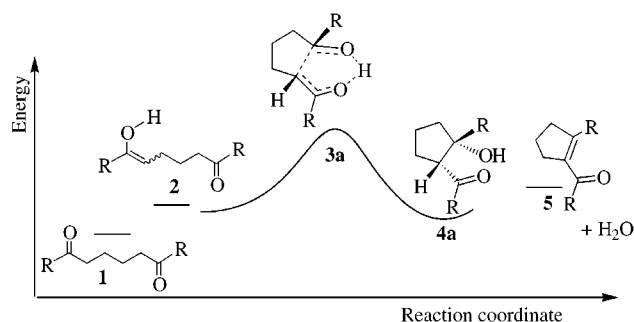


Figure 1. Qualitative reaction path a and numbering for the uncatalyzed mechanism. R can be either Me, SiH₃, *t*Bu, or TMS. A similar path, called path b, leads to the other diastereomer.

This computational study begins with detailed tests on the theoretical approximations. These method tests are usually meant to pick up a theoretical approximation appropriate to a problem. Of course, aiming to the study of systems as large as trimethylsilyl-disubstituted compounds, our choices are rather restricted by the computational cost. However, these tests will be helpful to analyze the reliability of the computational results. For the tests, all the structures of the uncatalyzed mechanism indicated in Figure 1 will be taken into account using the methyl substituted case (R = Me). They will be presented for both path a, which leads to **4a**, and path b, which leads to **4b**. The tests will be held on both the geometry optimization and the energy calculation. Our results for the uncatalyzed and the acid-catalyzed mechanisms will then be presented and discussed.

A. Tests on the Uncatalyzed Mechanism (R = Me). Figure 1 displays only the qualitative reaction path a for the uncatalyzed mechanism. As mentioned in Scheme 1, in the uncatalyzed path, the diketone **1** has first to enolize, leading to **2**. This enol can fold in a certain orientation to lead to the cyclic aldol product **4a** through a transition state noted **3a**. The last part of the Figure 1 concerns the dehydration of the aldol to the cyclopentenone **5**.

The methods we used are noted using the following convention: the Hartree–Fock method is noted HF, B3LYP¹⁰ method B3, and Moller–Plesset perturbation theory at the second-order MP2. An additional d label will indicate the use of the standard 6-31G(d) basis set while the absence of this d denotes the use of the standard 6-31G basis set. In the following, we will thus use HF for the HF/6-31G level, and B3d for B3LYP/6-31G(d). All the computations were done using the Gaussian¹¹ package. As indicated by former theoretical studies, a single reference wave function (HF or B3LYP) is appropriate to describe the aldol reactions.¹² The B3LYP method is even considered to be a very good choice for energy, geometry, and vibrations.¹³ The B3d level will be our reference in the following.

(10) (a) Lee, C.; Yang, W.; Parr, R. G. *Phys. Rev. B* **1988**, *37*, 7885. (b) Becke, A. D. *J. Chem. Phys.* **1993**, *98*, 5648.

(11) Gaussian 94 (Revision E.1 and E.2), Frisch, M. J.; Trucks, G. W.; Schlegel, H. B.; Gill, P. M. W.; Johnson, B. G.; Robb, M. A.; Cheeseman, J. R.; Keith, T. A.; Petersson, G. A.; Montgomery, J. A.; Raghavachari, K.; Al-Laham, M. A.; Zakrzewski, V. G.; Ortiz, J. V.; Foresman, J. B.; Peng, C. Y.; Ayala, P. A.; Wong, M. W.; Andres, J. L.; Replogle, E. S.; Gomperts, R.; Martin, R. L.; Fox, D. J.; Binkley, J. S.; Defrees, D. J.; Baker, J.; Stewart, J. P.; Head-Gordon, M.; Gonzalez, C.; Pople, J. A. Gaussian, Inc., Pittsburgh, PA, 1995.

(12) Bernardi, F.; Robb, M. A.; Suzzi-Valli, G.; Tagliavini, E.; Trombini, C.; Umani-Ronchi, A. *J. Org. Chem.* **1991**, *56*, 6472.

Table 2. Method Test at the HF/6-31G Optimized Geometry^a Unless Otherwise Specified.^b Absolute Energies (Hartree unless otherwise specified) for the Methyl-Substituted Systems (R = Me)

	HF	HFd	B3d	B3d ^b	stabilization ^c	MP2	MP2d
1	-460.62885	-460.83430	-463.73612	-463.73806	-1.2	-461.59564	-462.21689
2	-460.60829	-460.80174	-463.70707	-463.71031	-2.0	-461.56826	-462.18487
3a	-460.55631	-460.74436	-463.68148	-463.68445	-1.9	-461.54251	-462.16535
3b	-460.54624	-460.73492	-463.67395	-463.67717	-2.0	-461.53443	-462.15877
4a	-460.63122	-460.82509	-463.72764	-463.73147	-2.4	-461.59920	-462.22208
4b	-460.62594	-460.82013	-463.72300	-463.72648	-2.2	-461.59425	-462.21690
H ₂ O	-75.98536	-76.00968	-76.40695	-76.40895	-1.3	-76.11205	-76.19491
5	-384.62819	-384.78867	-387.29422	-387.29617	-1.2	-385.46710	-385.99360
H ₂ O+5	-460.61355	-460.79835	-463.70117	-463.70512	-2.5	-461.57915	-462.18851

^a HF, HFd, B3d, MP2, and MP2d stands for HF/6-31G, HF/6-31G(d), B3LYP/6-31G(d), MP2/6-31G, and MP2/6-31G(d) "Single Point" calculations, respectively. ^bB3LYP/6-31G(d) optimized geometry. ^cNet stabilization obtained by reoptimizing at the B3d level a geometry formerly obtained at the HF level (in kcal/mol, 1 Hartree = 627.5 kcal/mol).

Geometries. A first issue is to check the truthfulness of the HF geometries. Such a task can be done by analyzing the effect of a reoptimization at the B3d level of a structure formerly optimized at the HF level. The comparison could be done on the geometrical parameters, but it is much handier to discuss directly the energies obtained before and after the reoptimization (Table 2, stabilization^c = B3d^b - B3d). The reoptimization leads to a net stabilization of only about 2.0–2.5 kcal/mol in most cases, and 1.2 kcal/mol for the ketone. The HF (HF/6-31G) optimized geometries are thus in good agreement with the B3d (B3LYP/6-31G(d)) optimized geometries in our test case.

However, the lack of d orbitals for the Si atoms at the HF (HF/6-31G) level might introduce a larger error in our results when applied to the silylated substituted systems. This point has been tested using the energy difference between the silyl ketone **1** (R = SiH₃) and its aldol **4a** (R = SiH₃). For these systems, the reoptimization of **1** (R = SiH₃) and **4a** (R = SiH₃) from the HF level to the B3d level leads to a net stabilization of 0.9 and 2.4 kcal/mol, respectively. This shows a small dependence of the geometry to these factors (correlation and d orbitals), even for these silylated systems. These values are even extremely close to the one we obtained for the methyl-substituted ketone, and no special difficulties seem to be encountered for the theoretical description of these silylated systems. Finally, the HF geometries offer a good consistency along the reaction paths for both the Me and the SiH₃ substituted systems and will thus be our level of optimization for all this study.

Energies. The energies are usually more sensitive to the correlation than the geometries. This is of course the case here. HF and HFd levels are clearly not good enough to describe the correlation effects in the transition states. These methods find the transition states much too high in energy than better level. For instance, (Table 3) **3a** (R = Me) is about 50 kcal/mol higher in energy than **1** (R = Me) at these levels instead of about 33 kcal/mol at both MP2d and B3d levels. A special care must be used to calculate reliable energies. The B3d level will be used for this matter.

The main difference between the methods concerns finally the relative energies of the aldols. The diastereomer **4a** (R = Me) for instance is found 5 kcal/mol above the ketone **1** (R = Me) at the B3d level of approximation while the MP2 levels (both MP2 and MP2d) find it about 2 kcal/mol below the ketone. A discrepancy between the correlated levels is thus encountered, which indicates

Table 3. Relative Energies (kcal/mol) for the Methyl-Substituted Systems (R = Me) at the HF/6-31G Optimized Geometry^a Unless Otherwise Specified^b

	HF	HFd	B3d	B3d ^b	MP2	MP2d
1	0.0	0.0	0.0	0.0	0.0	0.0
2	12.9	20.4	18.2	17.4	17.2	20.1
3a	45.5	56.4	34.3	33.6	33.3	32.3
3b	51.8	62.4	39.0	38.2	38.4	36.5
4a	-1.5	5.8	5.3	4.1	-2.2	-3.3
4b	1.8	8.9	8.2	7.3	0.9	0.0
H ₂ O+5	9.6	22.6	21.9	20.7	10.4	17.8

^a HF, HFd, B3d, MP2, and MP2d stands for HF/6-31G, HF/6-31G(d), B3LYP/6-31G(d), MP2/6-31G, and MP2/6-31G(d) "Single Point" calculations, respectively. ^b B3LYP/6-31G(d) optimized geometries.

that one might not rely too much on these quantities. The energy for the dehydration, between H₂O + **5** (R = Me) and **4a** (R = Me), is also subject to caution as it appears to be both basis set¹⁴ and method¹⁵ dependent.

One might note however that the energy differences between the barriers are constantly reproduced at the correlated levels (B3d//HF, B3d//B3d, MP2//HF, and MP2d//HF): $\Delta E = 4.6 \pm 0.4$ kcal/mol is found between the two transition states **3a** (R = Me) and **3b** (R = Me). The same trend is observed for the energy difference between the aldols **4a** (R = Me) and **4b** (R = Me), the correlated methods converging to $\Delta E = 3.1 \pm 0.2$ kcal/mol. This consistency between the methods which are different in nature (DFT and Perturbation) is a good sign for the correctness of these quantities.

Our best compromise between the accuracy and the computational cost is thus the B3d//HF level of calculation, keeping in mind that (i) the energies between the paths a and b will be highly trustworthy (i.e., the energies between the transition states ΔE_{3b-3a} or between the aldols ΔE_{4b-4a}) and (ii) the relative energies of the aldols and of the dehydrated products might be subject to a larger error (for instance ΔE_{4a-1} and $\Delta E_{(H_2O+5)-4a}$). Nevertheless, while these quantities are expected to be less accurate, the results can be discussed qualitatively.

B. Results for the Uncatalyzed Mechanism (R = Me, SiH₃, Bu, TMS). Figure 2 displays the shape and few geometrical parameters obtained for these paths for the methyl substituent. The other substituents differ only slightly. All the information is given in Supporting Information. Selected geometrical parameters of the transition states for the different substituted systems are in Table 4, while Table 5 displays the energy results.

(14) Changing the basis set: the dehydration enthalpy is found at 12.6 and 21.1 kcal/mol at the MP2//HF and MP2d//HF, respectively.

(15) Changing the method: the dehydration enthalpy is found at 16.6 and 21.1 kcal/mol at the B3d//HF and MP2d//HF, respectively.

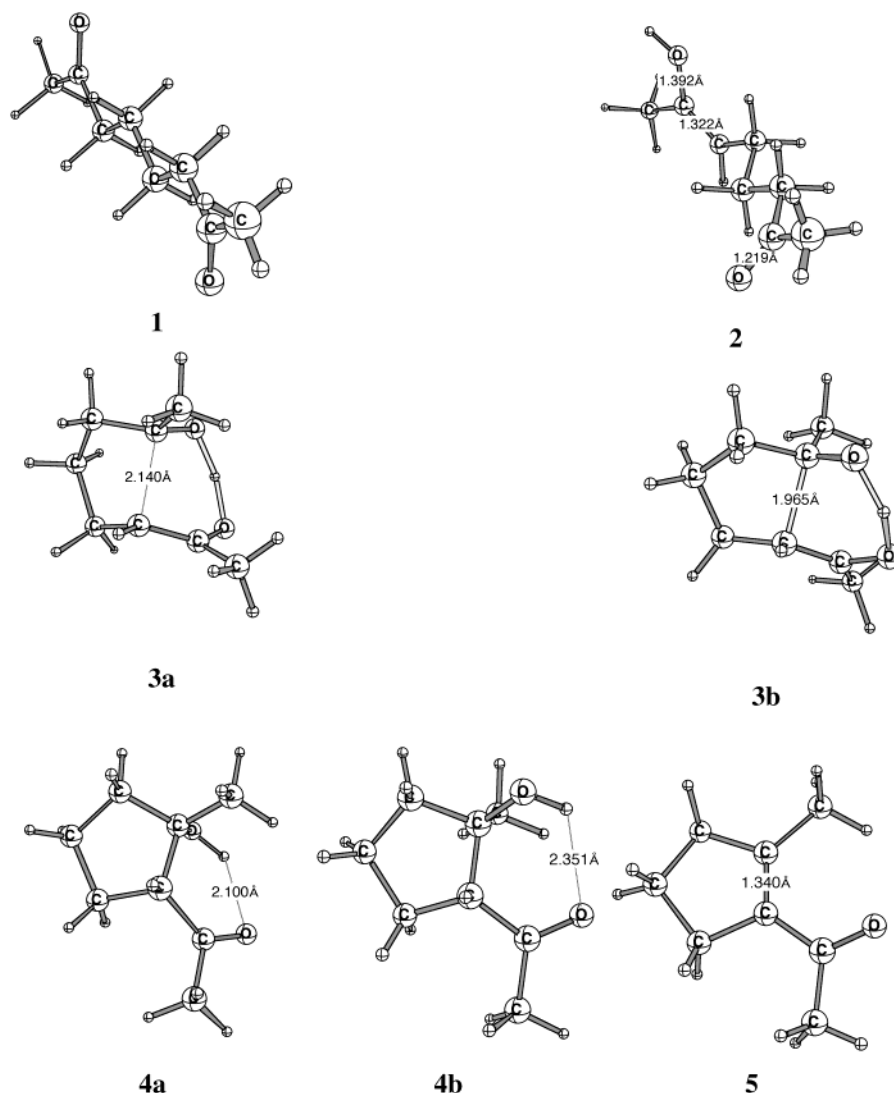
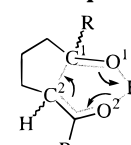


Figure 2. Shape of the HF optimized structures for the uncatalyzed mechanism ($R = \text{Me}$).

Table 4. Important Bond Lengths (Å) in the Transition States (uncatalyzed mechanism)

	3a				3b			
	Me	<i>t</i> Bu	SiH ₃	TMS	Me	<i>t</i> Bu	SiH ₃	TMS
C ¹ -C ²	2.140	2.294	2.268	2.303	1.965	1.973	1.970	1.927
O ¹ -H	1.220	1.169	1.155	1.151	1.330	1.391	1.319	1.384
O ² -H	1.186	1.222	1.255	1.254	1.127	1.081	1.135	1.095

A clear difference between the two transition states **3a** and **3b** lies in the progress of the C¹-C² bond formation with respect to the proton transfer from O² onto O¹: for the TS **3a**, the C¹-C² bond formation is late while the proton transfer is in an advance stage. Note for instance (Table 4) that in the TMS case (for **3a**), the proton transfer is almost completed: O¹-H is already as small as 1.151 Å while the C¹-C² distance is still at 2.303 Å. On the contrary for **3b** ($R = \text{TMS}$), the proton transfer appears to be "consecutive" to the C¹-C² bond formation.

The path a is found to be always preferred by ca. 5–13 kcal/mol in the transition state. This feature can be attributed to the hindrance of the substituent which disfavors the hydrogen bond in the path b. This point is

Table 5. Energies of the Uncatalyzed Mechanism, Relative (kcal/mol) to the Ketone Absolute Value (au)

B3d//HF	Me	<i>t</i> Bu	SiH ₃	TMS
1	-463.73612	-699.61322	-966.46504	-1202.42993
2	18.2	18.7	13.4	13.8
3a	34.3	38.2	30.1	32.5
3b	39.0	50.9	36.5	41.4
4a	5.3	11.6	3.9	7.6
4b	8.2	21.1	6.2	9.8
H ₂ O+5	21.9	30.4	13.7	17.1
ΔE_{3b-3a}	4.7	12.7	6.4	9.0
ΔE_{4b-4a}	2.9	9.5	2.3	2.2

well shown by the energy difference ΔE_{3b-3a} (Table 5). In the aldol products **4a** and **4b**, the selectivity is

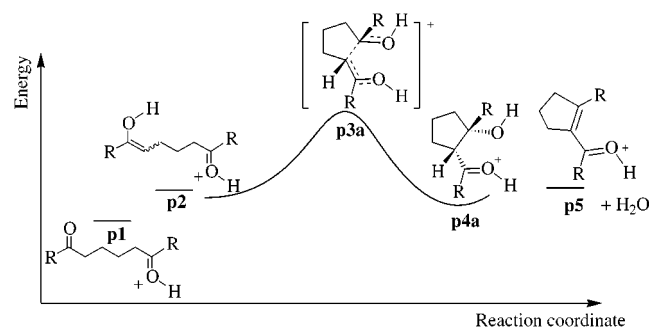


Figure 3. Qualitative reaction path a and numbering for the acid-catalyzed mechanism. R can be either Me, SiH₃, ^tBu, or TMS. A similar path, called path b, leads to the other diastereomer **p4b** (see text).

diminished as the energy difference becomes smaller ($\Delta E_{ab-4a} \sim 2$ kcal/mol, except for the ^tBu-substituted system). Hence, no large electronic effects of the silylated systems appear to induce the selectivity with respect to the alkylated systems.

While they may be subject to caution, one might also briefly comment on the energies of the products **4a** and **4b** which are systematically higher in energy than the starting materials **1** ($\Delta H > 0$). The free energy variation ΔG is expected to be also positive because the entropy is expected to diminish during this aldol reaction which leads to a cyclic species ($\Delta S < 0$). The entropy contribution is thus also positive ($-T\Delta S > 0$) and increases the enthalpy trend.¹⁶

For the dehydration reaction (**4a** \rightarrow **5** + H₂O), a positive enthalpy is also encountered but can be overcome by the entropic factor: ΔS is now positive since the reaction concerns a dissociation (vide infra).

Finally, these proton-chelated aldol reactions are quite energetically demanding as shown by the calculated energies of the transition states, ca. 30–40 kcal/mol (Table 5). The above-mentioned so-called “spontaneous” aldol cyclization does not appear to be feasible in view of these computational results. As the role of the PTSA is important to enable an aldol reaction (Scheme 2), an acid-catalyzed mechanism should be by far more appropriate. Nevertheless, we believe that the comparison between the two mechanisms will provide interesting indications about the role of the catalysis. For instance, it will be of special interest to know how important is the acid catalysis in the different stages of the reaction (enol formation and cyclization).

C. Results for the Acid-Catalyzed Mechanism (R = Me, SiH₃, ^tBu, TMS). The structures of the acid-catalyzed mechanism have been calculated at the same level we used for the uncatalyzed mechanism. As no special difficulties are introduced when adding a proton to the previous system, the accuracy of the computational methods should be similar. The notation is similar to the one used for the uncatalyzed mechanism (Figure 1), but the protonated structures will be noted with the prefix p (Figure 3: **p1**, **p2**, **p3a**...).

An important difference with the uncatalyzed mechanism concerns the absence of proton transfer. This point is best exemplified in Scheme 3 where the reaction can be understood as a charge (+) transfer from O¹ onto O², and the corresponding electronic reorganization: the protonated carbonyl (O¹) becomes an alcohol, while the enol (O²) becomes a protonated carbonyl. In the transition

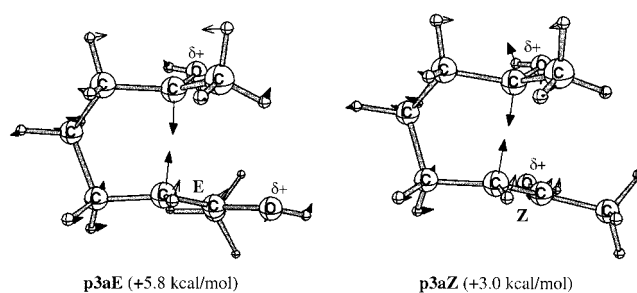
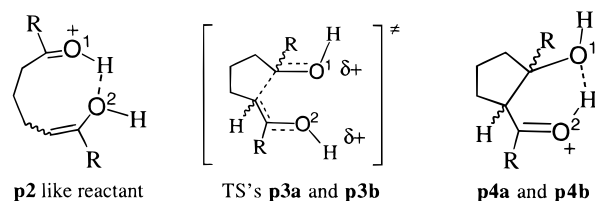


Figure 4. Two different transition state structures leading to the protonated aldol **p4a** (R = Me) in the methyl-substituted case (acid-catalyzed mechanism). The arrows indicate the reaction coordinate for the ring closure. The relative energy's origin is the protonated ketone **p1** (R = Me) (see Table 6).

Scheme 3



state, the charges are expected to display a behavior between the two situations, noted using the δ^+ charges in Scheme 3. A strong hydrogen bond can occur in the reactant between ⁺O¹–H (which bears a very positive proton) and O², while the hydrogen bond in the product concerns O¹ and H–⁺O².

In this context, where the protons must exchange their roles, it is well understood why we did not find a transition state with a hydrogen bond. However, a proton transfer could occur before or after the ring closure. These hypotheses have been tested in the methyl-substituted case but lead to unstable structures.¹⁷

Due to the absence of hydrogen bond in the transition state, the system gains more freedom and two kinds of transition state were searched for each path. As shown in Figure 4, they correspond to a simple *Z*–*E* isomerization of the enol's C=C bond. The difference in energy between the two transition state structures is of about 3 kcal/mol. For both paths a and b, the *Z*-like transition state were slightly preferred.

The shape and a few geometrical parameters obtained for these paths for the methyl substituent are displayed Figure 5. The other substituents differ only slightly, and the detailed structures can be found in the Supporting Information. The energies for the reaction under acid catalysis are now much lower than in the uncatalyzed mechanism. For instance, we find **p3aZ** (R = TMS) 6.3 kcal/mol (Table 6) higher than **p1** (R = TMS), while the corresponding TS **3a** (R = TMS) was 32.5 kcal/mol (Table 5) above **1** (R = TMS). The aldols **p4a** and **p4b** are now

(16) For the methyl case, the calculated values at the HF/6-31G level are $S = 115.4$ eu in **1** and 99.7 eu in **4a**, leading to $\Delta S = -15.8$ eu. Changing the pressure from 1 atm down to 10⁻⁵ atm changes the S , but not the ΔS . At $T = 300$ K, $\Delta S \sim -16$ eu leads to $-T\Delta S \sim +5$ kcal/mol.

(17) No minima were found at the HF level for a proton transfer before the ring closure. For a proton transfer after the ring closure, a transition state was found as well as the corresponding minimum. However the B3d single point calculations indicate an unstable compound (the reverse barrier disappeared). The HF result is thus artificial.

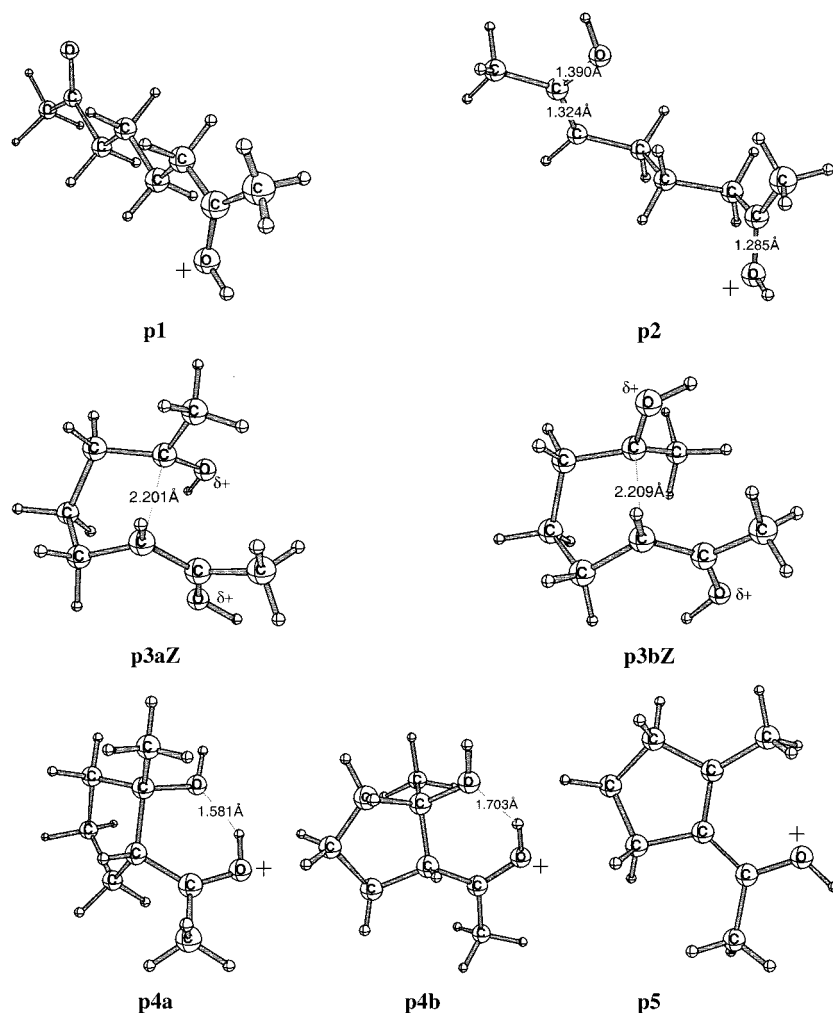


Figure 5. Shape of the lower HF optimized structures for the acid-catalyzed mechanism (R = Me).

Table 6. Energies of the Acid-Catalyzed Path, Relative (kcal/mol) to the Ketone Absolute Value (au)

B3d//HF	Me	<i>t</i> Bu	SiH ₃	TMS
p1	-464.06242	-699.95134	-966.78564	-1202.77198
p2	10.4	13.0	7.1	8.2
p3aZ	3.0	15.9	0.8	6.3
p3aE	5.8	18.5	3.7	8.0
p3bZ	6.2	19.5	3.5	9.4
p3bE	7.2	24.5	5.3	12.5
p4a	-12.1	-5.3	-12.8	-10.3
p4b	-6.8	6.3	-7.2	-2.9
H ₂ O+p5	4.1	19.2	0.0	4.2
$\Delta E_{p3bE-p3aZ}$	3.2	3.6	2.7	3.1
$\Delta E_{p4b-p4a}$	5.3	11.6	5.6	7.4

lower than the starting materials by 5 to 10 kcal/mol, except in the *t*Bu case (**p4b** (R = *t*Bu) = +6.3 kcal/mol).

Finally, the experimental selectivity is well described by the calculation, but is now more expressed in the aldols than in the transition states: the energy difference between the aldols **p4a** (R = TMS) and **p4b** (R = TMS) is now about 7.4 kcal/mol (Table 6), while this quantity amounts to only 3.1 kcal/mol between **p3aZ** (R = TMS) and **p3bE** (R = TMS).

Discussion

The computational study of the acid-catalyzed mechanism points out interesting indications for the reactivity of the different systems. One might in a first stage

consider the aldol formation and then discuss the dehydration step.

A. Aldol Formation. The significantly larger energy of the TS for the *t*Bu substituted derivative (Table 6, **p3aZ** = 15.9 kcal/mol) indicates a system less reactive toward the aldol reaction than in the others cases. As for the uncatalyzed mechanism, it can be attributed to the steric hindrance.

For the three other systems (R = Me, SiH₃, TMS), the **p3a** energies are not the limiting step but rather the formation of the enol **p2**. For instance, in the methyl-substituted case, **p2** (R = Me) is at 10.4 kcal/mol while the transition state **p3aZ** (R = Me) energy is only at 3.0 kcal/mol (Table 6). One might thus use the highest energies of **p2** and **p3a** in Table 6 for each system to analyze their reactivity. This leads to the following conclusions for the relative ease of reaction: SiH₃ (**p2** 7.1 kcal/mol), TMS (**p2** 8.2 kcal/mol), and Me (**p2** 10.4 kcal/mol). These conclusions are consistent with the fact that more vigorous conditions are necessary to undergo the aldol reaction with the methyl-substituted compounds (Table 1).

All the aldols **p4a** appear to be more stable than starting materials **p1**. For the Me derivative (Table 6) ΔH_{p4a-p1} is -12.1 kcal/mol. The corresponding modification of the entropy for the cyclization is calculated to amount to $\Delta S_{p4a-p1} = -16.8$ eu. It is interesting to note that for this Me-substituted system $\Delta G_{p4a-p1} = \Delta H_{p4a-p1}$

– $T\Delta S_{p4a-p1} = 0$ for a temperature $T = 720$ K (447 °C). ΔG is thus calculated to be negative below this (large) value ($T < 447$ °C).

For the ^tBu derivative, $\Delta H_{p4a-p1} = -5.3$ kcal/mol (Table 6), and assuming the same $\Delta S_{p4a-p1} = -16.8$ eu, one finds that the reaction bears a negative ΔG only for $T < 42$ °C.¹⁸ The same calculation for the TMS case leads to $T < 340$ °C, and for SiH₃ to $T < 489$ °C. Although these computed temperatures are only *estimated*, it is interesting to note the large difference between the ^tBu derivative and the other cases: The ^tBu derivative is theoretically not expected to undergo an aldol reaction if the temperature is too much over room temperature while a significantly higher temperature is allowed for the other cases. These results, combined with the necessary enolization energy, indicate an impossible aldolization of the ^tBu derivative.

B. Dehydration Step. Because acid-catalyzed dehydration is very fast, cyclopentenones **5** are the most frequently encountered products.^{1,2} Starting from the bis-(acylsilane) **1** (R = TMS), low yield (16%) of dehydrated product **5** (R = TMS) was obtained whereas the corresponding Me derivative **5** (R = Me) was the only compound detected and isolated (57%) (Scheme 2, Table 1: entries 1, 3). The preparation of the methyl-substituted cyclopentenone **5** (R = Me) was already mentioned in the literature using basic¹⁹ or acidic²⁰ media. Nevertheless, it is worth noting that intermediate aldol **4** (R = Me) was not detected for both reaction conditions.

The enthalpy to dehydrate from **p4a** to [**p5** + H₂O] is +16.2 and +14.5 kcal/mol for the Me and TMS systems, respectively (Table 6). The observed dehydration of both the Me- and TMS-substituted systems seems at a first glance to be in contradiction with these computed results which indicate a difficult dehydration from both systems. However, the calculation of ΔS for the dehydration of the methyl-substituted species leads to $\Delta S_{\text{dehydration}} = +41.2$ eu. It can be *estimated*²¹ that increasing the temperature should lead to the dehydrated cyclopentenone for temperatures over about 95 °C for the methyl-substituted systems and over about 55 °C for the TMS-substituted one. Due to possible error on the calculated enthalpies, the differences between the temperatures (~40 °C) is only indicative of a slightly easier dehydration of the TMS-substituted aldol. It is somewhat intriguing to note that in the preparative experiments (Table 1), the TMS aldol intermediate **4a** is mainly obtained, while the corresponding Me-substituted aldol is not observed because of the dehydration. The necessarily more vigorous experimental conditions (to increase the conversion) in the methyl-substituted systems can be a reason for this behavior.

To study the evolution of intermediates, we monitored the aldol condensation (heating near the indicated tem-

Table 7. Evolution of a Mixture of the Bis(acylsilane) and PTSA (10%) with Temperature

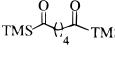
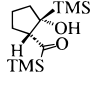
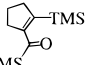
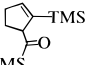
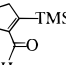
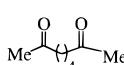
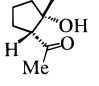
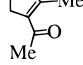
T (°C) (Time)					
35-40 (35 min.)	32%	58%	10%	-	-
60-65 (25 min.)	3%	10%	49%	38%	-
95-100 (30 min.)	-	-	64%	-	36%

Table 8. Evolution of a Mixture of Octane-2,7-dione and PTSA (10%) with Temperature

T (°C) (Time)			
35-40 (35 min.)	98%	-	2%
60-65 (25 min.)	78%	-	22%
95-100 (30 min.)	13%	-	87%

peratures the mixture of components under argon) by ¹H NMR analyses of successive aliquots of the crude mixture. The ratio of compounds are reported in Tables 7 and 8.

For the bis(acylsilane) (Table 7), at low temperature, the aldol **4a** (R = TMS) was the major product (58%) accompanied with a low yield of cyclopentenone **5** (R = TMS) (10%). At 60–65 °C, the cyclopentenone **5** (R = TMS) and its tautomer **6** were obtained in 49% and 38%, respectively. These two products were already obtained by mesylation of aldol **4a** (R = TMS) and treatment with triethylamine.⁷ At higher temperature, we observed the dehydrated product **5** (R = TMS) (64%) and the aldehyde **7** (36%) which was also mentioned in reference.⁷ For the methyl derivative (Table 8), we observed mainly diketone **1** (R = Me) at low temperature (35–40 °C). When the temperature was increased, the cyclopentenone **5** (R = Me) was formed exclusively. As it was the case in Table 1, no aldol was detected in the crude mixture.

From these observations (Tables 7 and 8), it seemed that the aldol reaction was easier with the bis(acylsilane) than with the methyl diketone. This point can be justified by the slightly easier bis(acylsilane) enol formation. In confirmation with the theoretical trends, the dehydration step was faster for the trimethylsilyl derivative (87% for **5** (R = TMS) + **6** against 22% for **5** (R = Me), at 60–65 °C). But at higher temperature, the methyl ketone gave a clean cyclocondensation (87% of **5** (R = Me)).

Conclusion

The bis(acylsilane) or its methyl analogue were easily converted, under acid activation, into the aldol **4a** or the corresponding α,β -unsaturated derivative **5**, respectively. For the bis(acylsilane), the aldol reaction is completely diastereoselective. The reasons for this selectivity were studied using two different mechanisms. For the uncatalyzed mechanism (Figure 1), the diastereoselectivity is expressed by the energy difference between the transition states and is thus subject to a kinetic control (Table 5:

(18) While the accuracy of ΔS is not extremely important, the accuracy of the ΔH is of crucial importance for the evaluation of these temperatures which must be handled with caution: the calculated ΔH might bear a small error with severe consequences on T . As usually, differences between the temperatures are more reliable than the temperatures themselves.

(19) Kossanyi, J. *Bull. Soc. Chim. Fr.* **1965**, 722.

(20) (a) Wiemann, J.; Thuan, S.-L. *Bull. Soc. Chim. Fr.* **1959**, 1537. (b) Kopecky, K. R.; Filby, J. E.; Mumford, C.; Lockwood, P. A.; Ding, J.-Y. *Can. J. Chem.* **1975**, *53*, 1103.

(21) Using the corresponding ΔH and assuming $\Delta S = +41.2$ eu for both the Me and the TMS-substituted systems, $\Delta G_{\text{dehydration}} = 0$ for $T = 393$ and 352 K for Me and TMS, respectively. Again, a small uncertainty on the ΔH can lead to severe consequences on the calculated temperatures.

ΔE_{3b-3a}) whereas, for the acid-catalyzed mechanism (Figure 3), it is better explained by the energy difference in the aldols (Table 6: $\Delta E_{p4b-p4a}$) and is thus under thermodynamic control. Both controls lead to the same diastereomer. In both mechanisms, the steric hindrance of the substituent seemed to be the main factor to induce the diastereoselectivity, rather than an electronic effect of the silyl group. The high energy barriers found in the uncatalyzed mechanism disagree with a spontaneous reaction in the refrigerator ($\Delta H_{3a} > 30$ kcal/mol). Residual acid must have been present in the samples.

Although it should be theoretically favored for the methyl derivative, no aldol reaction was observed during the reaction (Table 8). More vigorous conditions were required for the methyl-substituted system which led directly to the dehydrated product. The theoretical analysis brings the information of a limiting step at the enolization of the carbonyl function. Thus, it would be interesting to perform experimental and theoretical studies on unsaturated systems where the enolization would be favored through a conjugated enol. This aspect is currently under investigation.

Experimental Section

FT-IR spectra were run on a MIDAS Corporation apparatus. ^1H and ^{13}C NMR spectra were recorded on a Bruker AC-250 spectrometer. Tetramethylsilane ($\delta = 0.00$) or CHCl_3 ($\delta = 7.27$) were used as internal standards, and CDCl_3 was used as the solvent. The bis(acylsilane)⁷ and diketones **1** (R = Me),⁸ and **1** (R = 'Bu)⁹ were prepared according to the literature.

General Procedure for the Thermolysis with *p*-Toluenesulfonic Acid (PTSA). A mixture of diketone **1** (0.53 mmol, 1.0 equiv) and PTSA (0.1 equiv or 1.0 equiv) was heated (60–80 °C/ 2×10^{-2} mbar) in a Kugelrohr apparatus for 15 min. After cooling at room temperature, the crude was chromatographed over silica gel using mixture of petroleum ether/AcOEt as eluent to give the aldol **4a** or/and the cyclopentenones **5**.

Thermolysis of bis(acylsilane) 1 (R = TMS): see ref 7.

Thermolysis of Diketone 1 (R = Me). The thermolysis of diketone (75 mg, 0.53 mmol) and PTSA (100 mg, 1.0 equiv) gave, after chromatography over silica gel using petroleum ether/AcOEt (80/20), the cyclopentenone **5** (R = Me) (37 mg, 57%) and the starting diketone **1** (R = Me) (6 mg).

1-Acetyl-2-methylcyclopentenone. Oil. ^1H NMR: $\delta = 1.82$ (quint, $J = 7.6$ Hz, 2H), 2.09 (s, 3H), 2.25 (s, 3H), 2.50 (t, $J = 7.6$ Hz, 2H), 2.66 (m, 2H). ^{13}C NMR: $\delta = 16.7$ (CH_3), 21.3 (CH_2), 30.2 (CH_2), 34.2 (CH_2), 41.0 (CH_2), 135.6 (C_4), 154.1 (C_4), 198.3 (CO). IR (film): $\nu = 2921, 2853, 1678, 1657, 1615, 1356, 1260$ cm^{-1} .

Acknowledgment. The authors thank Dr. N. Hoffmann for valuable discussions. A substantial computational time allocation from the CRIHAN (Centre de Ressources Informatiques de HAute-Normandie) is gratefully acknowledged, project 1999010.

Supporting Information Available: Energies and XYZ coordinates for all the stationary points. This material is available free of charge via the Internet at <http://pubs.acs.org>.

JO005544Y